

Dynamics of Jaynes–Cummings Model in the Absence of Rotating-Wave Approximation*

FAN Yun-Xia,^{1,†} LIU Tao,¹ FENG Mang,^{1,2} and WANG Ke-Lin^{1,3}

¹School of Science, Southwest University of Science and Technology, Mianyang 621010, China

²State Key Laboratory of Magnetic Resonance and Atomic and Molecular Physics, Wuhan Institute of Physics and Mathematics, the Chinese Academy of Sciences, Wuhan 430070, China

³Department of Modern Physics, University of Science and Technology of China, Hefei 230026, China

(Received June 14, 2006)

Abstract *The Jaynes–Cummings model (JCM) is studied in the absence of the rotating-wave approximation (RWA) by a coherent-state expansion technique. In comparison with the previous paper in which the coherent-state expansion was performed only to the third order, we carry out in this paper a complete expansion to demonstrate exactly the dynamics of the JCM without the RWA. Our study gives a systematic method to solve the non-RWA problem, which would be useful in various physical systems, e.g., in a system with an ultracold trapped ion experiencing the running waves of lasers.*

PACS numbers: 03.65.-w

Key words: coherent-state expansion, rotating-wave approximation (RWA), Jaynes–Cummings model (JCM)

1 Introduction

The Jaynes–Cummings model (JCM),^[1] since its proposal, has been considered as a simple but very efficient description of a two-level system interacting with a single near-resonant quantum radiation. The model was first employed to investigate the classical aspects of the two-level system, and then extended to the quantum regime. It is generally believed today that the JCM is a useful tool to examine the basic properties of quantum electrodynamics (QED).^[2]

A number of remarkable properties of the JCM itself have drawn much attention, and have been successfully applied to the fundamental quantum theory of atoms under radiation of external fields, for example, the collapse and revival in the interaction of an atom with a field of coherent superposition, entanglement of the atom and the quantum field, and so on.^[3,4] Besides, the model has been generalized to multi-level systems experiencing multi-mode quantum fields.^[5] On the other hand, with the rapid development of cavity QED and laser technology, many state-of-the-art experiments have been performed for the possibility of a single atom confined in a single mode cavity^[6] or in an ion trap,^[7] for the single photon generation,^[8] and for preparation of macroscopic superposition states,^[9] which can be described by the JCM or by other extended models based on the idea of the JCM.

The RWA is from the energy conservation of the system involving an atom and the cavity mode.^[10] Previous studies have discovered that if we go beyond the RWA, i.e.,

introducing the additional terms, called counter-rotating terms, new features would appear, such as the chaotic behavior in the semiclassical treatment^[11] and the phenomena regarding the Bloch–Siegert shift in the quantum mechanical treatment.^[12] For an ion-trap system, a single ultracold trapped ion experiencing a laser radiation in the treatment of the JCM without the RWA is very different from that with the RWA when the system is moving to the strong excitation regime or going beyond the Lamb–Dicke regime.^[13,14]

The work in this paper is a generation of a previous solution^[15] in which the coherent-state expansion was only made to the third order. Although it is a systematic approach, the calculation made in Ref. [15] is only valid in short-time domain and in a narrow range of parameters. We will, in this paper, explore a complete expansion of the coherent-state and thus present an exact dynamics of the JCM in the absence of the RWA. Our main results include that (i) Wider range of parameters would be available in the calculation, which leads to remarkable discrepancy between RWA and non-RWA, and that (ii) the dynamics of a JCM could be demonstrated more exactly than in Ref. [15]. We have noticed that, in previous papers,^[13,14,16] the coherent-state techniques were employed to explore the eigenenergies and the eigenvectors of the JCM systems without the RWA. While compared with the time-independent solutions in Refs. [13], [14], and [16], the exactly dynamical properties presented in this paper

*The project supported by National Natural Science Foundation of China under Grant Nos. 10474118 and 10274093, the National Fundamental Research Program of China under Grant No. 2005CB724502, and the Foundation from Educational Department of Sichuan Province of China under Grant No. 2004C017

†E-mail: fanyunxia@swust.edu.cn

would be more useful for showing the importance of the non-RWA terms.

The paper is organized as follows. In Sec. 2, we will first check the validity of our coherent-state technique by solving the JCM under the RWA and then comparing with the standard solution. Our main result will be present in Sec. 3 in the treatment of a JCM without the RWA. The discussion and conclusion will appear in Sec. 4.

2 Solution Under RWA

The dimensionless Hamiltonian under our consideration is

$$\hat{H}_R = \frac{\Omega}{2}\sigma_z + a^\dagger a + g(a^\dagger\sigma_- + a\sigma_+), \quad (1)$$

where Ω is the transition frequency of the two levels, g is the coupling constant of the two levels to a quantum field with a^\dagger and a the corresponding creation and annihilation operators respectively, and $\sigma_{z,+,-}$ are usual Pauli operators. By using our coherent-state expansion technique, we suppose the trial solution of Eq. (1) to be

$$|t\rangle_{CA} = \begin{bmatrix} f_0(t) \\ h_0(t) \end{bmatrix} |A\rangle + \begin{bmatrix} f_1(t) \\ h_1(t) \end{bmatrix} a^\dagger |A\rangle + \begin{bmatrix} f_2(t) \\ h_2(t) \end{bmatrix} (a^\dagger)^2 |A\rangle + \cdots + \begin{bmatrix} f_n(t) \\ h_n(t) \end{bmatrix} (a^\dagger)^n |A\rangle, \quad (2)$$

where $|A\rangle = e^{\alpha_0 a^\dagger} |0\rangle$, $f_i(t)$ and $h_i(t)$ ($i = 0, 1, 2, \dots$) are time-dependent parameters to be determined later. After putting Eqs. (1) and (2) into Schrödinger equation

$$i\frac{\partial}{\partial t}|t\rangle = \hat{H}|t\rangle, \quad (3)$$

we compare the coefficients of $(a^\dagger)^m |A\rangle$ ($0 \leq m \leq n$) in both sides of the equation and obtain,

$$i\dot{f}_0(t) = \frac{\Omega}{2}f_0(t) + \alpha(t)gh_0(t) + gh_1(t), \quad (4a)$$

$$i[\dot{f}_m(t) + \dot{\alpha}(t)f_{m-1}(t)] = \frac{\Omega}{2}f_m(t) + \alpha(t)f_{m-1}(t) + mf_m(t) + \alpha(t)gh_m(t) + (m+1)gh_{m+1}(t) \quad (0 < m < n), \quad (4b)$$

$$i[\dot{f}_n(t) + \dot{\alpha}(t)f_{n-1}(t)] = \frac{\Omega}{2}f_n(t) + \alpha(t)f_{n-1}(t) + nf_n(t) + \alpha(t)gh_n(t), \quad (4c)$$

$$i\dot{h}_0(t) = -\frac{\Omega}{2}h_0(t), \quad (5a)$$

$$i[\dot{h}_m(t) + \dot{\alpha}(t)h_{m-1}(t)] = -\frac{\Omega}{2}h_m(t) + \alpha(t)h_{m-1}(t) + mh_m(t) + gf_{m-1}(t) \quad (0 < m \leq n). \quad (5b)$$

The occupation probability of the upper level is

$$P_{CA-1} = \sum_{i,j=0}^n \langle A|(a^\dagger)^i f_i^*(t) f_j(t) (a^\dagger)^j |A\rangle.$$

To check the validity of our solutions in Eqs. (4) and (5), we also solve it by a standard approach as demonstrated in Appendix. The two solutions are compared by numerical simulation, as shown in Figs. 1 ~ 3, where we suppose the initial state of the system to be in a coherent state

$$|t=0\rangle = \left(e^{\alpha_0 a^\dagger - \alpha_0^2/2} |0\rangle \right) = e^{-\alpha_0^2/2} \left(\sum_{n=0}^{\infty} \frac{\alpha_0^n}{\sqrt{n!}} |n\rangle \right)$$

with α_0 the initial number of bosons of the radiation field. We can see the very good agreement between the two solutions, which implies the validity of our approach of coherent-state expansion. As a result, from the next section, we will study the JCM in the absence of the RWA by this approach.

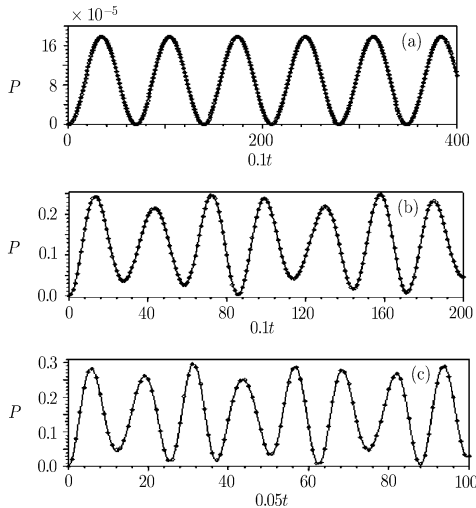


Fig. 1 Comparison of our method with the standard solution in the case of the RWA employed, where $\Omega = 0.1$, $\alpha_0 = 0.6$, and the dotted and solid curves represent our solution and the standard solution respectively. (a) $g = 0.01$; (b) $g = 1$; (c) $g = 5$.

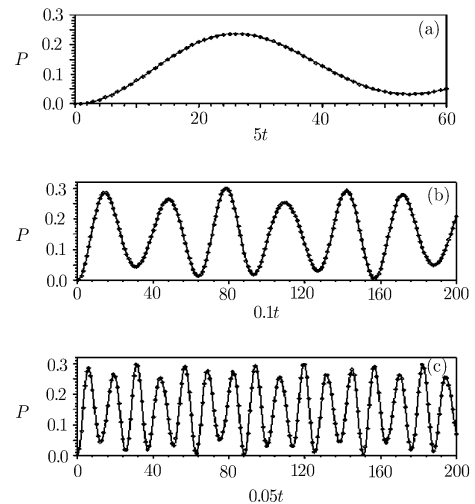


Fig. 2 Comparison of our method with the standard solution in the case of the RWA employed, where $\Omega = 0.99$, $\alpha_0 = 0.6$, and the dotted and solid curves represent our solution and the standard solution respectively. (a) $g = 0.01$; (b) $g = 1$; (c) $g = 5$.

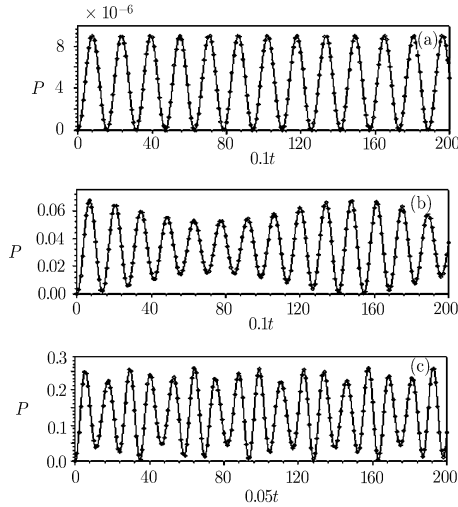


Fig. 3 Comparison of our method with the standard solution in the case of the RWA employed, where $\Omega = 5$, $\alpha_0 = 0.6$, and the dotted and solid curves represent our solution and the standard solution respectively. (a) $g = 0.01$; (b) $g = 1$; (c) $g = 5$.

3 Solution Without RWA

In the absence of the RWA, the counter-rotating terms should remain, which yields

$$\hat{H} = \frac{\Omega}{2}\sigma_z + a^\dagger a + g(a^\dagger + a)(\sigma_+ + \sigma_-). \quad (6)$$

By using the same trial solution as in Eq. (2), and repeating the steps in Sec. 2, we obtain the following equations:

$$i\dot{f}_0(t) = \frac{\Omega}{2}f_0(t) + \alpha(t)gh_0(t) + gh_1(t), \quad (7a)$$

$$i[\dot{f}_m(t) + \dot{\alpha}(t)f_{m-1}(t)] = \frac{\Omega}{2}f_m(t) + \alpha(t)f_{m-1}(t) + mf_m(t)$$

$$+ \alpha(t)gh_m(t) + (m + 1)gh_{m+1}(t) + gh_{m-1}(t) \quad (0 < m < n), \quad (7b)$$

$$i[\dot{f}_n(t) + \dot{\alpha}(t)f_{n-1}(t)] = \frac{\Omega}{2}f_n(t) + \alpha(t)f_{n-1}(t) + nf_n(t) + \alpha(t)gh_n(t) + gh_{n-1}(t), \quad (7c)$$

$$i\dot{h}_0(t) = -\frac{\Omega}{2}h_0(t) + \alpha(t)gf_0(t) + gf_1(t), \quad (8a)$$

$$i[\dot{h}_m(t) + \dot{\alpha}(t)h_{m-1}(t)] = -\frac{\Omega}{2}h_m(t) + \alpha(t)h_{m-1}(t) + mh_m(t) + \alpha(t)gf_m(t) + (m + 1)gf_{m+1}(t) + gf_{m-1}(t) \quad (0 < m < n), \quad (8b)$$

$$i[\dot{h}_n(t) + \dot{\alpha}(t)h_{n-1}(t)] = -\frac{\Omega}{2}h_n(t) + \alpha(t)h_{n-1}(t) + mh_n(t) + \alpha(t)gf_n(t) + gf_{n-1}(t), \quad (8c)$$

as well as the occupation probability

$$P_{CA-2} = \sum_{i,j=0}^n \langle A|(a)^i f_i^*(t) f_j(t) (a^+)^j |A\rangle$$

for the upper level.

4 Discussion and Conclusion

Figures 4 ~ 7 present the non-RWA solution for various cases. For convenience of our discussion below, we also plot the RWA solution based on the equations in Appendix. In the case of the large detuning, i.e., $\Omega \ll 1$ (Fig. 4) or $\Omega \gg 1$ (Fig. 7), the two solutions are very different, and the difference enhances with the increase of the coupling g . These results are in agreement with those in previous studies^[2-4] that the RWA is valid only in the case of near resonance and weak coupling.

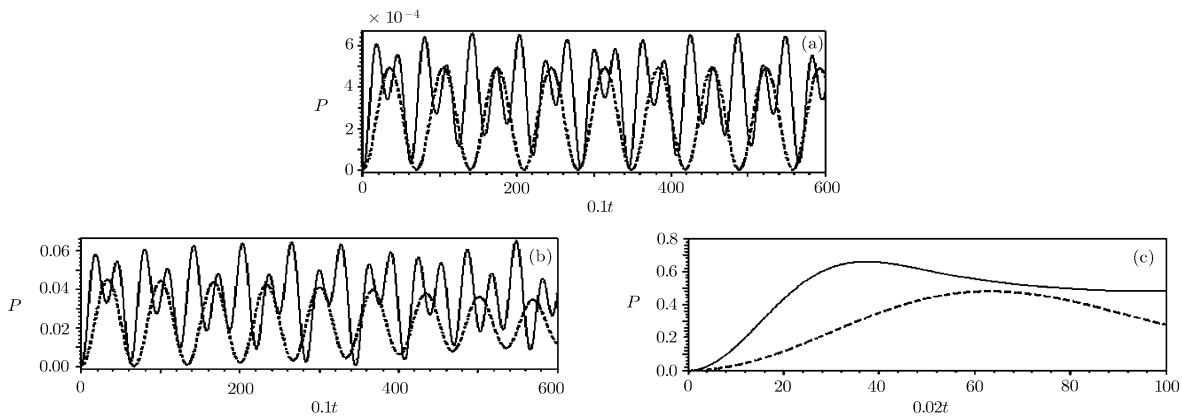


Fig. 4 In the large detuning case, our non-RWA solution versus g , where $\Omega = 0.1$, $\alpha_0 = 1$, and the solid and dashed curves represent our solution and the standard solution respectively. (a) $g = 0.01$; (b) $g = 0.1$; (c) $g = 0.9$.

Figure 6 presents the situation from the large detuning to the near-resonance, and to the large detuning again, from which we can see the changes by comparing the two solutions: from big difference to nearly agreement, and then to big difference again. To have more comparisons in the near-resonance case, we consider in Fig. 5 the change of the

coupling g . It is obvious that the difference between the non-RWA and the RWA in the weak coupling case is the small fluctuations with respect to the envelope. But the strong coupling would yield significant deviations in the figure.

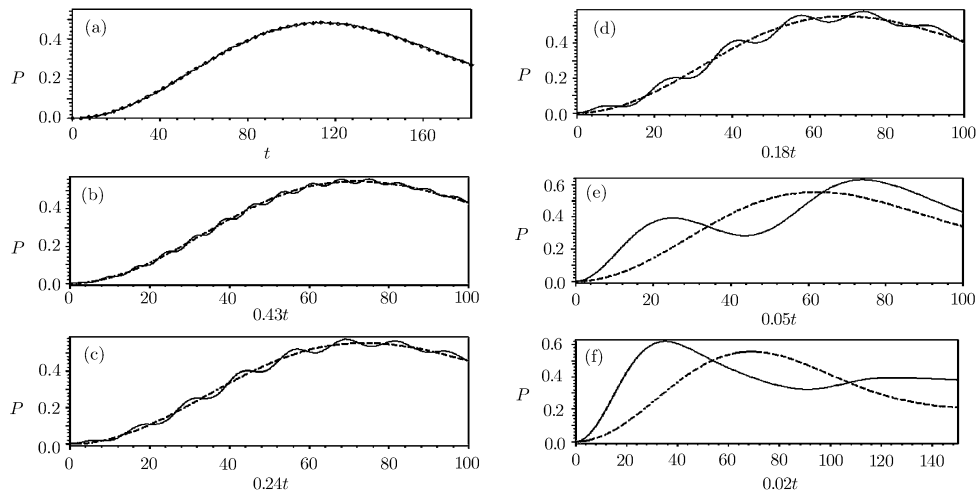


Fig. 5 In the case of near-resonance, our non-RWA solution versus g , where $\Omega = 0.99$, $\alpha_0 = 1$, and the solid and dashed curves represent our solution and the standard solution respectively. (a) $g = 0.01$; (b) $g = 0.04$; (c) $g = 0.07$; (d) $g = 0.1$; (e) $g = 0.4$; (f) $g = 0.9$.

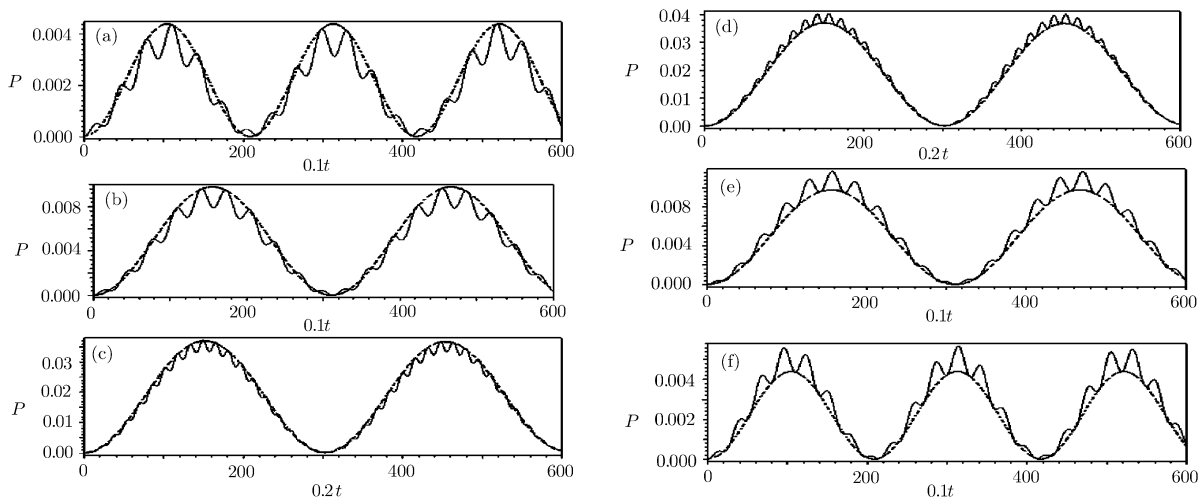


Fig. 6 In the case of weak coupling, our non-RWA solution versus Ω , where $g = 0.01$, $\alpha_0 = 1$, and solid and dashed curves represent our solution and the standard solution respectively. (a) $\Omega = 0.7$; (b) $\Omega = 0.8$; (c) $\Omega = 0.9$; (d) $\Omega = 1.1$; (e) $\Omega = 1.2$; (f) $\Omega = 1.3$.

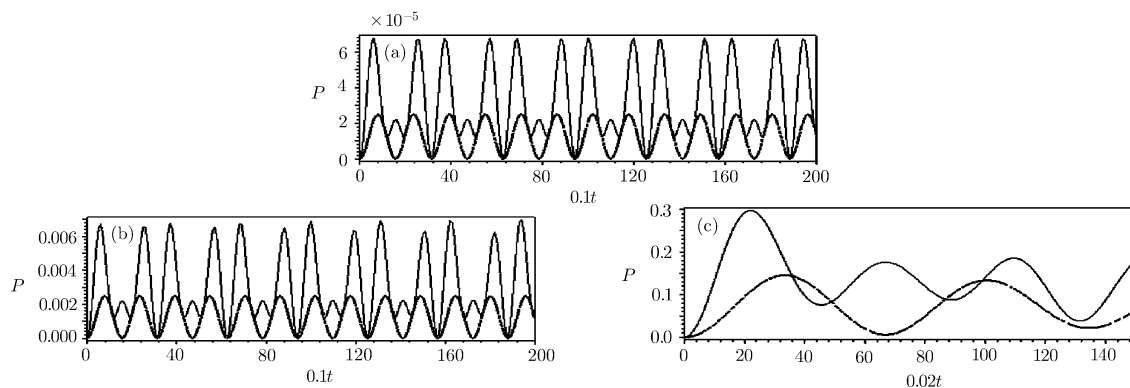


Fig. 7 In the large detuning case, our non-RWA solution versus g , where $\Omega = 5$, $\alpha_0 = 1$, and the solid and dashed curves represent our solution and the standard solution respectively. (a) $g = 0.01$; (b) $g = 0.1$; (c) $g = 0.9$.

Our non-RWA solution can be applied to many problems regarding two-level systems under the radiation. For example, for trapped ions experiencing traveling waves of lasers, the original Hamiltonian of the system can be unitarily transformed to^[13,14]

$$\hat{H} = \frac{\Omega}{2}\sigma_z + a^\dagger a + g(a^\dagger + a)(\sigma_+ + \sigma_-) + \varepsilon(\sigma_+ + \sigma_-) + g^2, \tag{9}$$

where the variables are of different physical meanings from those in Eq. (6): Ω is the laser-ion coupling constant, g is related to the Lamb–Dicke parameter, and ε is associated with the detuning of the lasers to the resonant transition of the two levels of the ion. If we consider a resonant case well within the Lamb–Dicke regime, i.e., $\varepsilon = 0$, and $g \ll 1$, equation (9) is reduced to Eq. (6). So our investigation in Sec. 3 actually treats such an ion trap problem. If we neglect the RWA solutions in Figs. 4 ~ 7, the figures could give us an impression that a single ion under the radiation of two counter-propagating traveling waves of lasers in the carrier transition ($\varepsilon = 0$) behaves in a complicated way even within the weak excitation ($\Omega < 1$) and the Lamb–Dicke ($g \ll 1$) regimes. This complicacy, overlooked in the RWA treatment, comes from the nonlinearity due to the exponential terms of $(a^\dagger + a)$ (See, for example, equation (1) in Ref. [13]).

As a systematic approach, our non-RWA solution could be applied to the investigation of the behavior of the trapped ions in the strong-excitation regime for both traveling and standing waves of the lasers, in which the coupling constant is larger than the trap frequency, i.e., $g > 1$ in Eq. (6), and the RWA is definitely invalid in this situation. The strong-excitation regime was employed in quantum state preparation and quantum information processing^[17–19] due to the advantage of fast operation, which is very helpful in view of decoherence. In this sense, our approach as well as the results would be useful for more careful consideration of these schemes.

In summary, we have presented an exact dynamics of JCM in the absence of the RWA by a complete expansion of the coherent-state. The validity of the RWA was examined specifically under different parameters by the comparison between the RWA and non-RWA solutions. In contrast to the approximate solutions in Ref. [15], we have demonstrated an exact time-evolution of a JCM in a wide range of parameters, in the absence of the RWA. We argue that our systematic approach could be applied to various problems regarding JCM without the RWA.

Appendix:

We present here the standard approach to the solution of Eq. (1) by assuming $|t\rangle = \sum_0^\infty \begin{bmatrix} a_n(t)|n\rangle \\ b_n(t)|n+1\rangle \end{bmatrix}$ to be the trial solution, where $a_n(t)$ and $b_n(t)$ are to be determined. From the Schrödinger equation (3), we have,

$$i \sum_0^\infty \begin{bmatrix} \dot{a}_n(t)|n\rangle \\ \dot{b}_n(t)|n+1\rangle \end{bmatrix} = \sum_0^\infty \begin{bmatrix} \left[\frac{\Omega}{2}a_n(t) + na_n(t) + g\sqrt{n+1}b_n(t)\right]|n\rangle \\ \left[-\frac{\Omega}{2}b_n(t) + (n+1)b_n(t) + g\sqrt{n+1}a_n(t)\right]|n+1\rangle \end{bmatrix}. \tag{A1}$$

Setting $a_n(t) = A_n e^{i\omega_n t}$ and $b_n(t) = B_n e^{i\omega_n t}$ with A_n, B_n and ω_n being constant coefficients to be solved later, we get to two simple equations,

$$\left(\frac{\Omega}{2} + n + \omega_n\right)A_n + g\sqrt{n+1}B_n = 0, \tag{A2}$$

$$\left(-\frac{\Omega}{2} + n + 1 + \omega_n\right)B_n + g\sqrt{n+1}A_n = 0. \tag{A3}$$

The non-zero solutions of A_n and B_n are determined by

$$\begin{vmatrix} \frac{\Omega}{2} + n + \omega_n & g\sqrt{n+1} \\ g\sqrt{n+1} & -\frac{\Omega}{2} + n + 1 + \omega_n \end{vmatrix} = 0, \tag{A4}$$

from which we obtain

$$\omega_n^{(1,2)} = -\left(n + \frac{1}{2}\right) \pm \frac{\sqrt{(\Omega - 1)^2 + 4g^2(n+1)}}{2}. \tag{A5}$$

So the time-dependent coefficients in Eq. (A1) are $a_n(t) = A_n^{(1)} e^{i\omega_n^{(1)}t} + A_n^{(2)} e^{i\omega_n^{(2)}t}$ and $b_n(t) = B_n^{(1)} e^{i\omega_n^{(1)}t} + B_n^{(2)} e^{i\omega_n^{(2)}t}$. We assume the system to be initially in the lower component of the two levels and in a coherent quantum field, i.e.,

$$|t=0\rangle = \begin{pmatrix} 0 \\ e^{\alpha_0 a^\dagger - \alpha_0^2/2}|0\rangle \end{pmatrix} = e^{-\alpha_0^2/2} \begin{pmatrix} 0 \\ \sum_{n=0}^\infty \frac{\alpha_0^n}{\sqrt{n!}}|n\rangle \end{pmatrix} = \sum_0^\infty \begin{bmatrix} a_n(0)|n\rangle \\ b_n(0)|n+1\rangle \end{bmatrix} = \sum_0^\infty \begin{bmatrix} (A_n^{(1)} + A_n^{(2)})|n\rangle \\ (B_n^{(1)} + B_n^{(2)})|n+1\rangle \end{bmatrix}. \tag{A6}$$

From Eqs. (A2), (A3), and (A6), we can have the solution

$$A_n^{(1)} = -\frac{g}{\omega_n^{(1)} - \omega_n^{(2)}} \frac{\alpha_0^{n+1} e^{-\alpha_0^2/2}}{\sqrt{n!}}, \tag{A7}$$

$$A_n^{(2)} = \frac{g}{\omega_n^{(1)} - \omega_n^{(2)}} \frac{\alpha_0^{n+1} e^{-\alpha_0^2/2}}{\sqrt{n!}}, \tag{A8}$$

$$B_n^{(1)} = \frac{\frac{\Omega}{2} + n + \omega_n^{(1)}}{\omega_n^{(1)} - \omega_n^{(2)}} \frac{\alpha_0^{n+1} e^{-\alpha_0^2/2}}{\sqrt{(n+1)!}}, \quad (\text{A9})$$

$$B_n^{(2)} = -\frac{\frac{\Omega}{2} + n + \omega_n^{(2)}}{\omega_n^{(1)} - \omega_n^{(2)}} \frac{\alpha_0^{n+1} e^{-\alpha_0^2/2}}{\sqrt{(n+1)!}}, \quad (\text{A10})$$

and the occupation probability of the upper level is

$$\begin{aligned} P_R(t) &= \sum_{n,m=0}^{\infty} \langle n|a_n^*(t)a_m(t)|m\rangle = e^{-\alpha_0^2} \sum_{n=0}^{\infty} \{A_n^{(1)2} + A_n^{(2)2} + 2A_n^{(1)}A_n^{(2)} \cos[(\omega_n^{(2)} - \omega_n^{(1)}) \cdot t]\} \\ &= -2g^2 e^{-\alpha_0^2} \left\{ \sum_{n=0}^{\infty} \frac{\alpha_0^{2n+2} [-1 + \cos(\sqrt{\Omega^2 - 2\Omega + 1 + 4g^2n + 4g^2} \cdot t)]}{(\Omega^2 - 2\Omega + 1 + 4g^2n + 4g^2)n!} \right\}. \end{aligned} \quad (\text{A11})$$

References

- [1] E.T. Jaynes and F.W. Cummings, Proc. IEEE **51** (1963) 89.
- [2] S. Stenholm, Phys. Rep. **6** (1973) 1.
- [3] B.W. Shore and P.L. Knight, J. Mod. Opt. **40** (1993) 1195.
- [4] For example, J.H. Eberly, N.B. Narozhny, and J.J. Sanchez-Mondragon, Phys. Rev. Lett. **44** (1980) 1323.
- [5] M. Tavis and F.W. Cummings, Phys. Rev. **170** (1968) 379.
- [6] J.M. Raimond, M. Brune, and S. Haroche, Rev. Mod. Phys. **73** (2001) 565.
- [7] D. Leibfried, R. Blatt, C. Monroe, and D. Wineland, Rev. Mod. Phys. **75** (2003) 181.
- [8] M. Keller, B. Lange, K. Hayasaka, W. Lange, and H. Walther, Nature (London) **431** (2004) 1075.
- [9] C. Monroe, D.M. Meekhof, B.E. King, and D.J. Wineland, Science **272** (1996) 1131.
- [10] Here we consider the RWA from the viewpoint of a single particle process. Actually the RWA can also be understood as an average effect, in which counter-rotating terms only result in virtual excitations and thereby counteract with each other. So nothing is observable associated with the counter-rotating terms. However, in ion-trap systems, the blue-detuning is a real physical process, which is resulted by counter-rotating terms if we treat the system by JCM. This special case is due to the external source of lasers which are treated classically.
- [11] P.W. Milonni, J.R. Ackerhalt, and H.W. Galbraith, Phys. Rev. Lett. **50** (1983) 966.
- [12] L. Armstrong and S. Feneuille, J. Phys. B **6** (1973) L182.
- [13] M. Feng, X. Zhu, X. Fang, M. Yan, and L. Shi, J. Phys. B **32** (1999) 701.
- [14] M. Feng, Eur. Phys. J. D **18** (2002) 371.
- [15] Z.J. Zhang, K.L. Wang, and G. Qin, Chin. Phys. **14** (2005) 1317.
- [16] G. Qin, K.L. Wang, T.Z. Li, R.S. Han, and M. Feng, Phys. Lett. A **239** (1998) 272.
- [17] S.B. Zheng, X.W. Zhu, and M. Feng, Phys. Rev. A **62** (2000) 033807.
- [18] J.F. Poyatos, J.I. Cirac, and P. Zoller, Phys. Rev. Lett. **81** (1998) 1322.
- [19] M. Feng, Euro. Phys. J. D. **29** (2004) 189.